

# Uni-Traveling-Carrier Balanced Photodiode with Tunable MMI Coupler for Optimization of Source Laser RIN Suppression

Jonathan Klamkin\*, Anand Ramaswamy, Leif A. Johansson, Nobuhiro Nunoya,  
John E. Bowers, Steven P. DenBaars, Larry A. Coldren  
Materials Department and Electrical and Computer Engineering Department  
University of California, Santa Barbara, CA USA

\*Now with Lincoln Laboratory, Massachusetts Institute of Technology, Lexington, MA USA  
Email: klamkin@ll.mit.edu

**Abstract**—A balanced uni-traveling-carrier (UTC) waveguide photodiode (PD) has been fabricated and characterized. The balanced PD incorporates a multimode interference (MMI) coupler as a light combiner/splitter with tunability of the output power splitting ratio. The individual UTC-PDs demonstrate a 1 dB compression current of 80.5 mA and a third-order output intercept point of 46.1 dBm at 60 mA, both representing the highest reported for a waveguide PD. The ability to fine tune the output power splitting of the MMI coupler allows for optimization of source laser relative-intensity noise suppression.

## I. INTRODUCTION

Balanced photodiodes (BPDs) are used in a number of systems including microwave photonic links and coherent communications systems [1], [2], [3]. In microwave photonic links, differential detection with a BPD can be used to suppress relative-intensity noise (RIN) leading to a lower overall noise figure and improved dynamic range. To optimize the RIN suppression, the photodiodes (PDs) in the BPD pair should be precisely matched both electrically and optically, and the incident optical power on each PD should be equal. Also for high dynamic range microwave photonic links, such as that in [4], it is desirable that the PDs demonstrate a high 1 dB compression current and high third-order output intercept point (OIP3).

We previously demonstrated the concept of current injection tuning in a multimode interference (MMI) coupler/splitter in a BPD in [5]. The output power splitting tunability of the MMI coupler allows for optimization of source laser RIN suppression, and increased fabrication and fiber alignment tolerances. The PDs, which were uni-traveling-carrier PDs (UTC-PDs) demonstrated a 1 dB compression current of greater than 40 mA and OIP3 of 43 dBm at 20 mA and 34 dBm at 40 mA. Here we have optimized the design of the tunable MMI coupler and significantly improved the performance of the UTC-PDs. The coupler can be fine tuned with low levels of injected current while exhibiting low excess loss over a broad wavelength range. The individual UTC-PDs demonstrate a 1 dB compression current of 80.5 mA and a OIP3 of 46.1 dBm at 60 mA and 44.2 dBm at 80 mA. These represent the highest

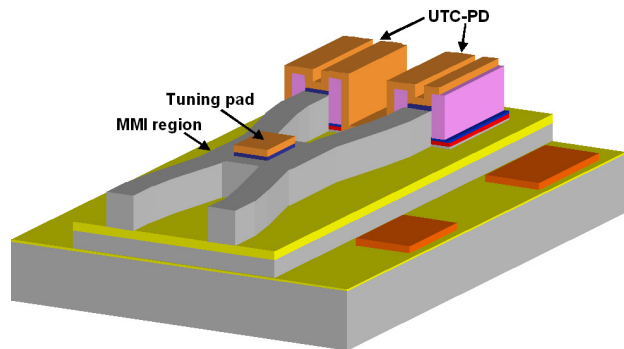


Fig. 1. Plan view schematic of UTC-BPD.

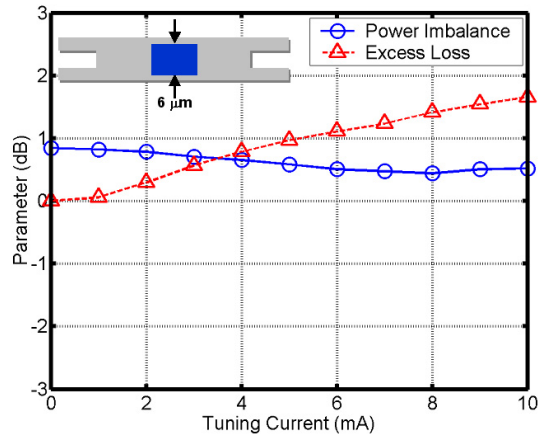
reported 1 dB compression current and OIP3 for a waveguide PD. In the balanced configuration, the OIP3 is subsequently 52.1 dBm and 50.2 dBm at 60 mA and 80 mA respectively.

## II. BALANCED PHOTODIODE DESIGN AND FABRICATION

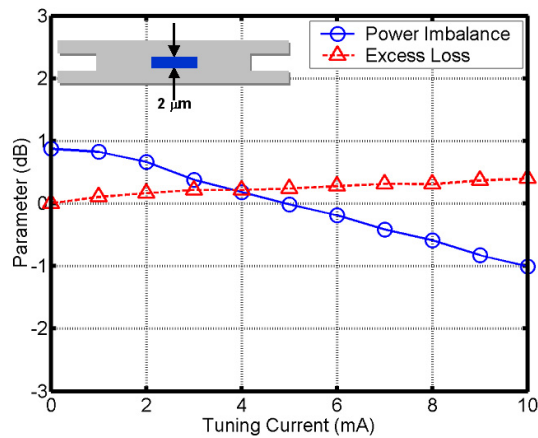
The waveguide BPD, shown in Fig. 1, consists of a pair of high power UTC-PDs, a compact tunable MMI coupler/splitter, and additional passive interconnection elements including waveguide bends and tapers. The UTC-PD structure sits on top of an *InGaAsP* waveguide layer. The monolithic integration fabrication sequence consisted of a photodetection region formation step followed by a p-cladding and p-contact layer regrowth step. The components were all fabricated in a surface ridge architecture. The structure was grown on a semi-insulating *InP* substrate. To realize the balanced configuration, the two adjacent waveguide UTC-PDs were electrically isolated using etching and a high energy ion implantation technique, and subsequently connected in series using a monolithic metal interconnect.

### A. Tunable Multimode Interference Coupler

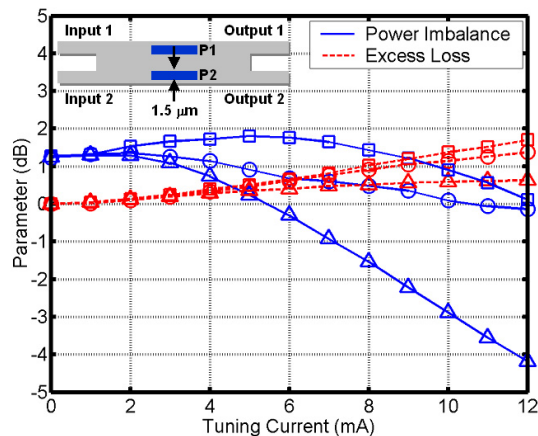
The coupler used was a general interference MMI coupler. The imaging length of a MMI coupler is extremely sensitive to the multimode region width [6]. Additionally, the imaging characteristics are dependent on the excitation at the input



(a) Design 1. The tuning pad is  $100\ \mu\text{m}$  long,  $6\ \mu\text{m}$  wide, and is placed in the center of the MMI region.



(b) Design 2. The tuning pad is  $100\ \mu\text{m}$  long,  $2\ \mu\text{m}$  wide, and is placed in the center of the MMI region.



(c) Design 3. The tuning pads are each  $100\ \mu\text{m}$  long,  $1.5\ \mu\text{m}$  wide, and are placed in the center of the MMI region along the length and  $1\ \mu\text{m}$  from the edges along the width.

Fig. 2. Power imbalance and excess loss as a function of tuning current for the three different tuning pad geometries.

of the multimode region, which can be altered by fiber coupling misalignment. MMI couplers with tunable output power splitting ratios can increase the design, fabrication, and fiber alignment tolerances for devices that require well-defined splitting ratios [7]. Tunable MMI couplers can also be used for fine tuning the output power splitting ratio. This allows for optimization of source laser RIN suppression in a BPD.

Tuning the splitting of a MMI coupler exploits the fact that within the multimode region, the input field is reproduced in single or multiple images at periodic intervals along the direction of propagation. The interference of the self-images at one interval leads to the formation of new self-images at the next interval. By modifying the refractive index locally within one interval where self-images occur, the phase relations between the self-images at the next interval will be changed thereby altering the final output images.

A straightforward way to realize a tunable MMI coupler is to change the refractive index in locations where the most distinct self-images occur such as halfway along the length of the MMI. With a beam propagation method simulation, the lateral positions of these self-images at the halfway point can be identified by the points with high field intensity. If the refractive index near the middle two self-images is changed with respect to the refractive index near the outer two self-images, or vice-versa, the output power splitting ratio will be altered.

The refractive index of the material within the MMI can be changed in a number of ways including carrier-induced techniques such as the plasma effect, which leads to a negative refractive index change [8], [9]. Reasonable refractive index changes can be achieved with only modest carrier densities therefore fairly low levels of free carrier absorption are induced, which would otherwise reduce the net tuning effect in the MMI coupler. In order to inject carriers and tune the refractive index, a metal contact pad was integrated as shown in Fig. 1.

Tuning pads with three different geometries were fabricated and characterized. In all cases the length of the tuning pad was  $100\ \mu\text{m}$  where the total MMI region length was  $350\ \mu\text{m}$ , and the tuning pads were placed in the center along the length of the MMI region. The width of the MMI region was  $8\ \mu\text{m}$ . Design 1 incorporated a single tuning pad that was  $6\ \mu\text{m}$  wide and placed in the center of the MMI region along the width. Design 2 incorporated a single tuning pad that was  $2\ \mu\text{m}$  wide and identically placed. Lastly, design 3 incorporated two  $1.5\ \mu\text{m}$  wide tuning pads placed  $1\ \mu\text{m}$  from the edges so that the spacing between the contacts was  $3\ \mu\text{m}$ .

### B. Uni-Traveling Carrier Photodiode

The UTC-PD was utilized because this type of PD demonstrates both high speed and high current operation [10]. In a UTC-PD light is absorbed in an undepleted p-type narrow bandgap layer (absorber) and photogenerated electrons subsequently diffuse to a wide bandgap drift layer (collector). Because electrons are the only active carriers and electrons have a higher drift velocity than holes, space charge saturation

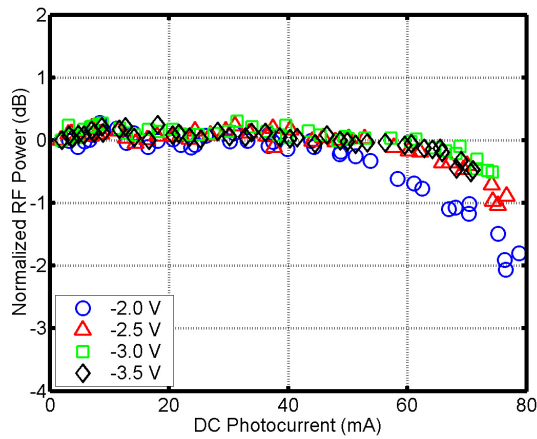


Fig. 3. Normalized RF power as a function of DC photocurrent at 1 GHz for varying bias voltages. The data is normalized to an ideal line with a slope of 20 dB/decade.

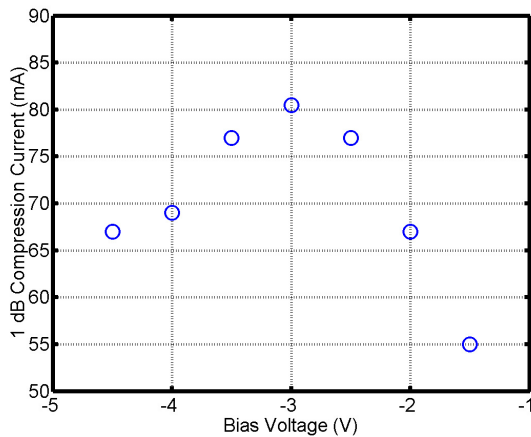


Fig. 4. 1 dB compression current as a function of bias voltage at 1 GHz.

effects are reduced in comparison to a traditional PIN photodiode (PD).

The UTC-PD structures were grown above the *InGaAsP* optical waveguide core and passive regions were formed by selectively removing the PD layers. The thickness of the field termination layer, a highly n-doped *InP* layer between the waveguide and PD layers, could be tailored to adjust the overlap of the optical mode with the absorber layer. A lower overlap factor results in a longer absorption profile and in turn a more uniform distribution of generated photocarriers along the length of the PD. This reduces the space charge saturation at the front end and improves the overall performance. As long as the field termination layer is not made considerably thick, only a slight increase in series resistance would be incurred in increasing the thickness of this layer.

The UTC-PDs used in the BPD have a p-*InGaAs* absorber that is 75 nm thick and is uniformly doped to a concentration of  $4\text{E}18\text{ cm}^{-3}$ , an *InP* collector that is 200 nm thick and is unintentionally doped, and a n-*InP* field termination layer

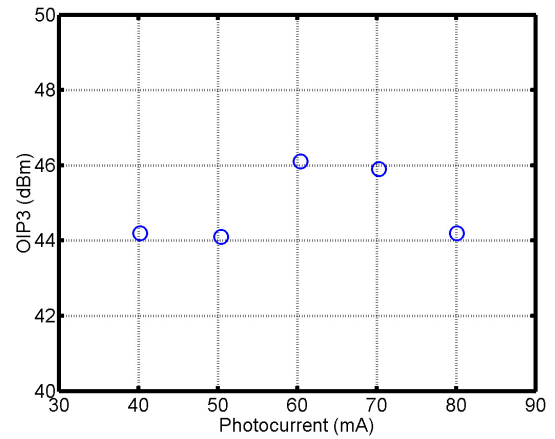


Fig. 5. Two-tone OIP3 as a function of photocurrent level.

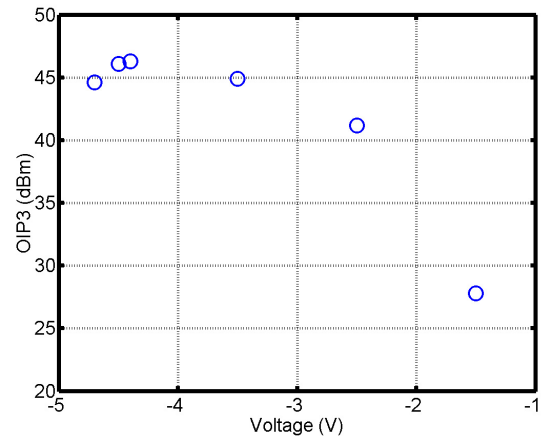


Fig. 6. Two-tone OIP3 as a function of bias voltage for a photocurrent level of 60 mA.

that is 70 nm thick and is doped to a concentration of  $2\text{E}18\text{ cm}^{-3}$ .

### III. RESULTS AND DISCUSSION

For the MMI couplers, 50:50 splitting was achieved over a wide wavelength range. To test the tuning properties of the MMI couplers, the fiber was intentionally misaligned to force an imbalance with a magnitude of around 1 dB with no current injected, and then current was injected to tune to a power imbalance of 0 dB. Here the power imbalance is defined as  $10\log(P_{OUT2}/P_{OUT1})$ . The imbalance was measured with light coupled to one input access waveguide.

Figure 2 shows the measured power imbalance and excess loss as a function of tuning current for all three MMI tuning pad designs. The excess loss is the excess total transmission loss incurred as a result of increasing the tuning current and modifying the splitting properties of the MMI coupler. With the fiber misaligned, the excess loss increased with tuning current for all of the designs. Recall that these MMI couplers performed optimally with no current injected. The intentional

misalignment of the fiber changed the excitation at the input to the MMI region. The purpose of this experiment was to simulate a fiber misalignment for a packaged device, and test the viability of tuning the MMI splitting with current injection using the different tunable MMI designs. This situation could also simulate a BPD with PDs that are not identical.

For design 1, the splitting improved as the injected current was increased, however 50:50 splitting, or a power imbalance of 0 dB, was not achieved within the current range applied. Additionally, the excess loss was fairly significant. For design 2, with 5 mA of current, the splitting was tuned to a power imbalance of 0 dB from an imbalance with a magnitude slightly less than 1 dB while very little excess loss was induced. For design 3, with two tuning pads, current could be injected into each pad simultaneously, or into one pad only. In Fig. 2(c), the input and output access waveguides and the contact pads are labeled. Light was coupled to input 1 only and the fiber was misaligned so that a larger fraction of the output power was measured at output 2, and the power imbalance was slightly greater than 1 dB. Current was then injected into contact pad P2 only (circles in the figure), P1 only (triangles in the figure), and into both pads simultaneously (squares in the figure). For current injected into P2 only, the power imbalance could be tuned to 0 dB, however 12 mA of current was required and greater than 1 dB of excess loss was induced. For current into P1 only, the power imbalance could be tuned to 0 dB with only 5.4 mA of current and less than 0.5 dB of excess loss. For current into both P1 and P2, the power imbalance initially increased and then decreased to 0 dB at a current of 12 mA.

To characterize the UTC-PDs, the 1 dB compression current and OIP3 were measured. The 1 dB compression current was measured at various biases. Fig. 3 shows the normalized RF power as a function of DC photocurrent at 1 GHz. The response is fairly flat to greater than 60 mA and then begins to decrease gradually. The 1 dB compression current for this PD is 80.5 mA at a bias of -3.0 V. This high compression current is attributed to the low front-end saturation resulting from the relatively thick field termination layer. Figure 4 shows the 1 dB compression current as a function of bias voltage. The 1 dB compression current reaches a maximum at -3.0 V.

Third-order intermodulation distortion (IMD3) measurements were carried out using a three-tone setup as in [11]. For these measurements the fundamental frequencies used were  $f_1 = 980$  MHz,  $f_2 = 1$  GHz, and  $f_3 = 1.015$  GHz. Figure 5 shows the two-tone OIP3 as a function of DC photocurrent. At 60 mA and a bias of -4.5 V, the OIP3 was 46.1 dBm. This is the highest reported OIP3 for a WG-PD. Although high at all the measured photocurrent levels, the OIP3 was highest at 60 mA. The OIP3 at 80 mA, the highest photocurrent level measured, was 44.2 dBm with a bias of -3.6 V. The bias was lowered at 80 mA to prevent thermal runaway. Figure 6 shows the two-tone OIP3 as a function of bias voltage at a photocurrent level of 60 mA. The OIP3 is highest at a bias of -4.4 V, and remains higher than 40 dBm for biases as low as -2.5 V. At a bias of -1.5 V, the OIP3 drops below 30 dBm.

#### IV. CONCLUSIONS

We have demonstrated a UTC-BPD with a tunable MMI coupler for fine tuning the output power splitting ratio. With a carefully designed tuning pad geometry, the power imbalance can be tuned from 1 dB to 0 dB with little excess loss. The UTC-PDs demonstrate a 1 dB compression current of 80.5 mA and a OIP3 of 46.1 dBm at 60 mA and 44.2 dBm at 80 mA. The 1 dB compression current and the OIP3 values represent the highest reported for a waveguide PD.

#### ACKNOWLEDGMENT

This research was supported by the DARPA PHOR-FRONT program under United States Air Force contract number FA8750-05-C-0265.

#### REFERENCES

- [1] T. E. Darcie and A. Moye, "Modulation-Dependent Limits to Intensity-Noise Suppression in Microwave-Photonic Links," *IEEE Photonics Technology Letters*, vol. 17, pp. 2185–2187, 2005.
- [2] P. J. Winzer and H. Kim, "Degradations in Balanced DPSK Receivers," *IEEE Photonics Technology Letters*, vol. 15, pp. 1282–1284, 2003.
- [3] A. Joshi, D. Becker, C. Wree, and D. Mohr, "Coherent Optical Receiver System with Balanced Photodetection," in *Proc. of SPIE*, vol. 6243, 2006.
- [4] J. Klamkin, L. A. Johansson, A. Ramaswamy, J. E. Bowers, S. P. Denbaars, and L. A. Coldren, "Monolithically integrated coherent receiver for highly linear microwave photonic links," in *IEEE Lasers and Electro-optics Conference*, 2007.
- [5] J. Klamkin, A. Ramaswamy, H.-F. Chou, M. N. Sysak, J. W. Raring, N. Parthasarathy, S. P. DenBaars, J. E. Bowers, and L. A. Coldren, "Monolithically integrated balanced uni-traveling-carrier photodiode with tunable MMI coupler for microwave photonic circuits," in *Conference on Optoelectronic and Microelectronic Materials and Devices*, 2006.
- [6] L. B. Soldano and E. C. M. Pennings, "Optical Multi-Mode Interference Devices Based on Self-Imaging: Principles and Applications," *Journal of Lightwave Technology*, vol. 13, pp. 615–627, 1995.
- [7] J. Leuthold and C. H. Joyner, "Multimode Interference Couplers with Tunable Power Splitting Ratios," *Journal of Lightwave Technology*, vol. 19, pp. 700–707, 2001.
- [8] B. R. Bennett, R. A. Soref, and J. A. D. Alamo, "Carrier-Induced Change in Refractive Index of InP, GaAs, and InGaAsP," *IEEE Journal of Quantum Electronics*, vol. 26, pp. 113–122, 1990.
- [9] J.-P. Weber, "Optimization of the Carrier-Induced Effective Index Change in InGaAsP Waveguides—Application to Tunable Bragg Filters," *IEEE Journal of Quantum Electronics*, vol. 30, pp. 1801–1816, 1994.
- [10] T. Ishibashi, T. Furuta, H. Fushimi, S. Kodama, H. Ito, T. Nagatsuma, N. Shimizu, and Y. Miyamoto, "InP/InGaAs Uni-Traveling-Carrier Photodiodes," *IEICE Transactions on Electronics*, vol. E83-C, no. 6, pp. 938–949, June 2000.
- [11] A. Ramaswamy, J. Klamkin, N. Nunoya, L. A. Johansson, L. A. Coldren, and J. E. Bowers, "Three-Tone Characterization of High-Linearity Waveguide Uni-Traveling-Carrier Photodiodes," in *IEEE Lasers and Electro-Optics Society Conference*, 2008.